Astronomical and Astrophysical Transactions (*AApTr*), 2019, Vol. 31, Issue 2, pp. 147–158,
ISSN 1055-6796, Photocopying permitted by license only, ©Cambridge Scientific Publishers

Nonstationary processes in the active region on the Sun before, during, and after the LDE-flare

A.N. Shakhovskaya[1,*], I.Yu. Grigoryeva[2], E.A. Isayeva[3]

[1] *Crimean Astrophysical Observatory RAS, Nauchny, Republic of Crimea, Russia*
[2] *Main Astronomical (Pulkovo) Observatory RAS, St.-Petersburg, Russia*
[3] *Radio Astronomy Observatory URAN-4, Odessa, Ukraine*

Received 1 October, 2018

The events that took place on September 24, 2011, in the active region (AR) NOAA 11302 are investigated. The Hα observations of the CrAO, the RSTN radio observations, and the results of the EUV-line space observations are used. In this AR there was the LDE-flare, we also studied in detail the events preceding and following this flare. It is known that in the AR there was a complex magnetic configuration as a result of emergence of new bipolar spots between the tail and the leading spot of it. A system of low loops intertwined with each other was formed above these spots. East of the tail spot and west of the leading spot there are high loops along which the eruption of EUV jets occurs. As a result of eruptive processes, a powerful Coronal Mass Ejection (CME) is formed, and a settling matter after which contributes to the development of the LDE-flare in low loops and subsequent flares without a significant CME.

Keywords: LDE-flares, Hα emission, EUV jets, type III bursts, corona, CME

1 Introduction

There is a great variety of powerful flares, however, two significantly different classes can be distinguished, namely compact or pulsed flares and Long Duration Events (LDEs). The most important criterion for their difference is the duration of the flare in the soft X-ray emission. In this paper we use the model proposed in Gopalswamy (2003) and Grechnev et al. (2006). Schematically, powerful nonstationary processes on the Sun can be represented as follows: the development of the instability of the MHD configuration leads to the ejection of a solar substance that opens a part of the closed magnetic field lines. Subsequent relaxation causes the magnetic force line reconnection, with the appearance of a coronal current sheet. At some point, the onset of a prolonged phenomenon leads to pulsed energy release and the subsequent formation of coronal loops filled with hot plasma. Its soft X-ray emission in some

*Email: anshakh@yandex.ru

cases lasts 10–20 minutes, while in others it slowly decays for many hours. In short X-ray flares a free flaring of hot plasma occurs. Such flares are often called compact. LDE-flares are characterized by the formation of a post-eruptive large-scale arcade. In this paper, the events preceding and following the LDE-flare that occurred on September 24, 2011 at 12:33 UT, in the photosphere, the chromosphere, and the corona are investigated.

2 Observations of the active region NOAA 11302

In the present study, the following data are used: the original filtergrams carried out with the small CrAO coronagraph (KG-1: Babin 1974) and observations of the *Large Angle Spectroscopic Coronagraph* (LASCO: Brueckner et al. 1995) onboard the *Solar and Heliospheric Observatory* (SOHO); solar images from the *Atmospheric Imaging Assembly* (AIA: Lemen et al. 2012) and photospheric magnetograms produced by the *Helioseismic and Magnetic Imager* (HMI: Scherrer et al. 2012) onboard the *Solar Dynamic Observatory* (SDO); EUVI 195 Å images of the *Extreme Ultraviolet Imager* (EUVI: Howard et al. 2008) onboard STEREO-B spacecraft of the twin *Solar Terrestrial Relations Observatory* (STEREO: Kaiser et al. 2008); radio data from the *Radio Solar Telescope Network* (RSTN: Guidice 1979; Guidice et al. 1981) and the measurement of the integrated flux of the Sun in soft X-ray from the GOES-15 satellite.

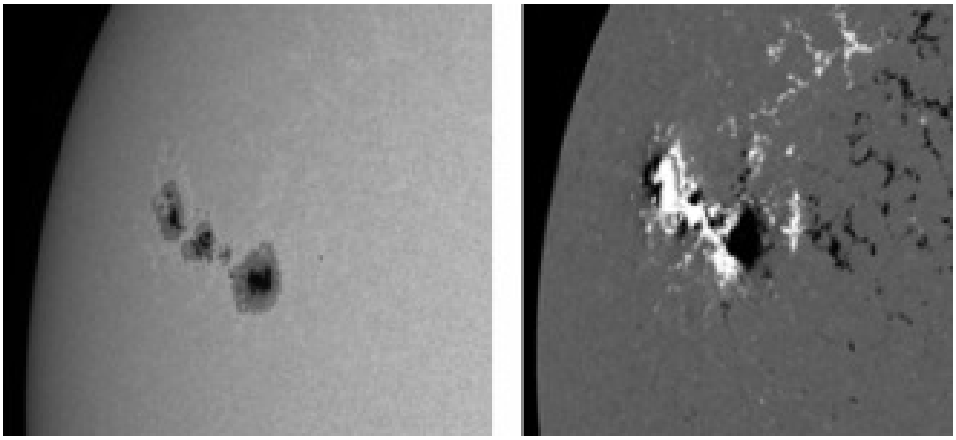


Figure 1 On the left, the White Light filtergram of the AR NOAA 11302 and on the right, the light of site magnetogram obtained by the SDO/HMI in on September 24, 2011 at 12:00 UT.

The first maximum of cycle 24 occurred in September 2011. The AR NOAA 11302 was the largest in area and was characterized by the highest flare activity. The maximum size of the AR was 1300 parts per million (ppm) of the solar disk hemisphere on September 25, the most powerful X1.9 flare was observed on 24 September from

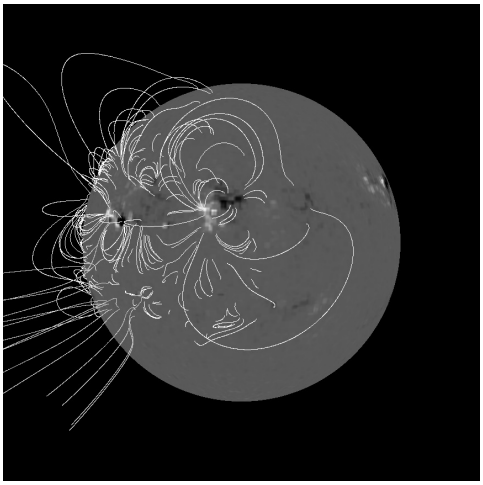


Figure 2 The direction of the force lines of the potential magnetic field in the corona, calculated in the PFSS approximation in September 24, 2011 at 12:04 UT is superimposed on the image of the magnetic field (SDO/HMI).

09:21 UT. In this paper, we investigate the M7.1 X-ray flare, which occurred on September 24, 2011 with the onset of soft X-ray at 12:33 UT, the peak at 13:20 UT and the end at 14:10 UT according to the GOES data. Thus, its total duration is more than 1.5 hours (97 minutes), which allows it to be considered an LDE-flare, according to the GOES data. It was on the disk from September 22 to October 04, 2011, during this time there were 2 X-ray flares of the X class, 14 – M class and 34 flares of the C class. Of the large number of sufficiently powerful flares, only two of them can be considered LDEs. One of them occurred on September 22, 2011, when the AR was still on the Eastern limb, and the other – on September 24, 2011 at 12:30 UT. Our work is devoted to the LDE-flare, which occurred on September 24, 2011 when the AR was in the rise phase with the magnetic configuration of $\beta\gamma$ and the next day – $\beta\gamma\delta$ quadrupolar-type configuration. The position on the disk of this AR, corresponding to the coordinates N12E56 at the moment of the LDE-flare being studied, is shown in Fig. 1. On this day, sun spots of this AR can be divided into 3 parts: leading, central and tail, and in each of them there are spots of different polarities.

The spots of different polarity in the tail are particularly close to each other, and "magnetic flux canceling" takes place here (Wang, Shi 1993). We used the Potential Field Source Surface (PFSS) model from the SolarSoft package provided by the Lockheed Martin Solar and Astrophysics Laboratory (LMSAL: www.lmsal.com/∼derosa/pfsspack/). The force lines of the potential magnetic field in the corona, calculated in the PFSS approximation, visible in Fig. 2 east of the tail spots, close behind the eastern limb, and in the southeast they form an open configuration.

In the image obtained by the STEREO-B spacecraft in 195 Å line, we can see the coronal hole located in the south-east of the AR, and to the east – another AR (see Fig. 3).

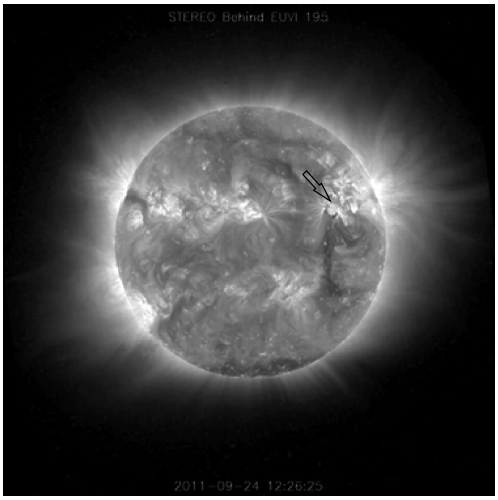


Figure 3 The image of the full solar disk, received by STEREO-B in the 195 Å line on September 24, 2011 at 12:26 UT, where the AR NOAA 11302 is shown by the contour arrow.

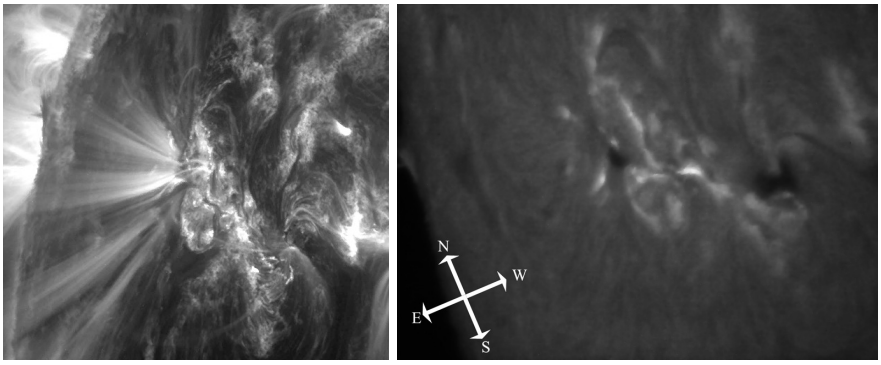


Figure 4 On the left, the AR 11302 image obtained by SDO/AIA in 171 Å line on September 24, 2011 at 12:26 UT. On the right, the Hα line filtergram of the same AR and time (telescope KG-1, CrAO), the arrow cross in the left bottom corner shows directions on the solar disk.

Frequently erupting EUV jets both before and after the LDE-flare are observed above the spots in the tail part of the AR, where spots of different polarity are most closely located and magnetic flux is canceled. These jets are best observed in the 304 Å line (SDO/AIA), and they are directed along the force lines and coronal loops, to the east and to the southeast (see Fig. 5). EUV jets are accompanied by type III radio bursts. Hα serge corresponding to EUV jets before LDE-flare is very weak, but after it at 15:40 UT there is a bright Hα surge or a subflare.

According to Hα and EUV line observations, the rope is observed from twisted loops of different brightness (see Fig. 4). Repeated flares visible on images in the

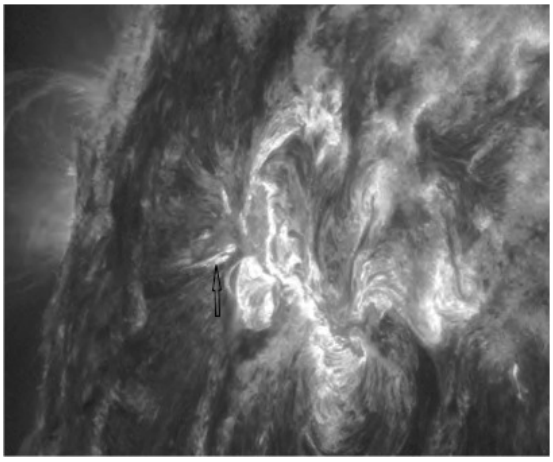


Figure 5 The AR 11302 image obtained in the 304 Å line (SDO/AIA) on September 24, 2011 at 12:26 UT, the arrow shows EUV jet.

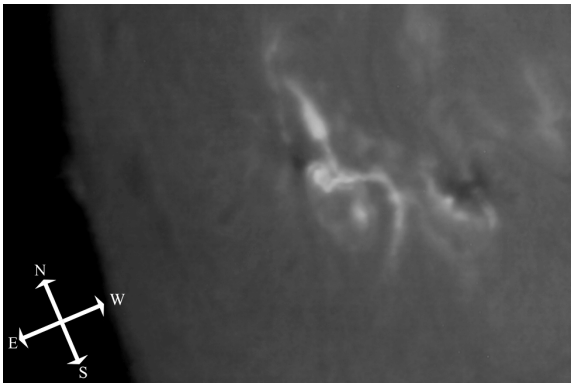


Figure 6 The filtergram of the AR at 12:50 UT in the Hα line obtained by the KG-1 telescope (CrAO).The arrow cross in the left bottom corner shows directions on the solar disk.

Hα line (KG-1, CrAO) and in 1600 Å line (SDO/AIA) occurred above the central sunspots in the AR in this rope (Fig. 6).

High-energy CMEs with a large mass, whose direction corresponds to the direction of the jets (to the south and south-east), were associated with LDE-flares on September 22 and 24, 2011. For the LDE-flare on September 24, the CME was in the form of a partial halo (see Figs 7, 8). Its mass and kinetic energy were $1.6e + 16$ grams and $3.0e + 32$ ergs, respectively. This is an order of magnitude higher than the average. As can be seen from Figs 7, 8, the CME consisted of two initially independent parts. The eastern part began in a broad solid angle, and the southeast can be called a coronal jet which was the continuation of the EUV jet. Subsequently, we see

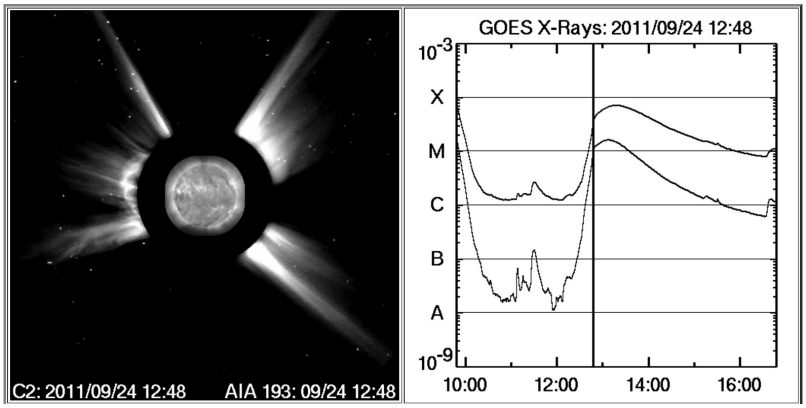


Figure 7 On the left, the first occurrence of the CME associated with LDE-flare observed by SOHO LASSO/C2. On the right, the soft X-ray flux with the GOES-15 spacecraft, taken from the site https: //cdaw.gsfc.nasa.gov/CME_list/daily_movies/2011/09/24/00_movie_matrix.html (see the left top link – the combined movie "C2AIA+X-ray").

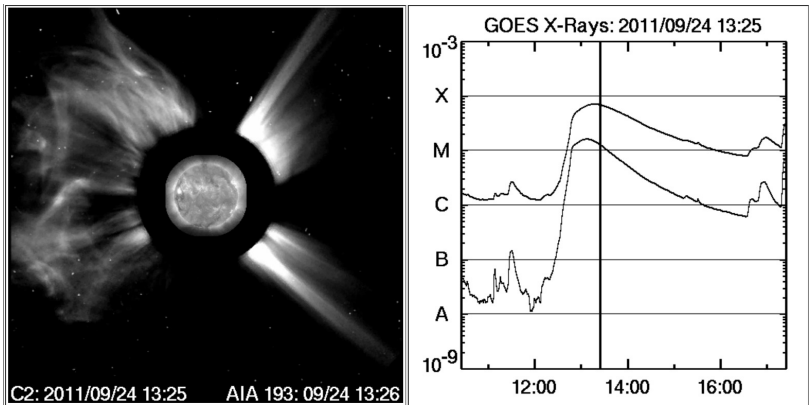


Figure 8 The image of the CME (LASSO/C2) in the form of the partial halo taken from SOHO LASCO CME CATALOG from the same link as Fig. 7.

that the south-eastern part of the CME also took a wide solid angle and merged with the eastern, at least visually. CMEs associated with other flares in this AR were of less mass and energy.

3 The timeline of events related to the LDE-flare September 24, 2011

According to SOHO LASCO CME CATALOG (https://cdaw.gsfc.nasa.gov/) the first CME registration in the field of view of LASCO/C2 was at 12:48 UT. In Bain et al.

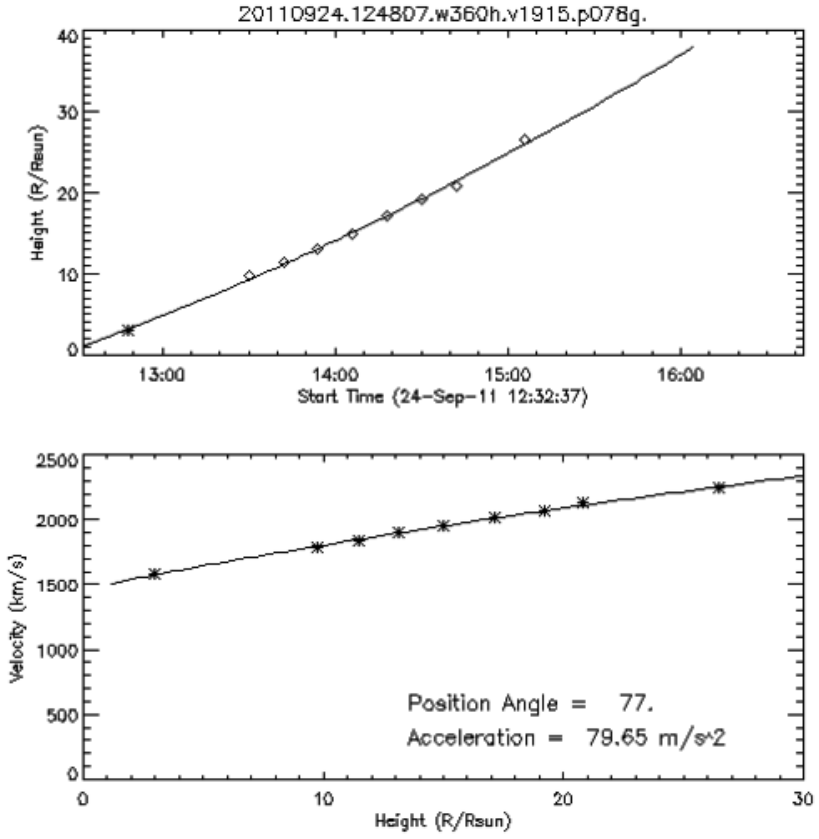


Figure 9 Light curves of height and velocity of the CME on September 24, 2011 obtained by second-order extrapolation (https://cdaw.gsfc.nasa.gov/).

(2012) it is shown that the start time of the CME, calculated by extrapolation, can be as before, or after the beginning of the X-ray flare. However, most often these times coincide with the accuracy of the measurement error. So in our case, it is about 12:30 UT (see Fig. 9). Thus, the flare investigated by us was recorded in soft X-ray (GOES) almost simultaneously with the CME event.

The soft X-ray flare according to the GOES data began at 12:32 UT, and type III radio bursts were recorded at 12:26 UT (RSTN). In order to determine the initial time of the jets and the flare visible in the chromospheric lines, we chose as a jet marker the brightness of its footpoint observed in the 1600 Å line (SDO/AIA). However, this brightness appears somewhat later than the jet observed in the 304 Å line. We identified some two areas in the AR image in the 1600 Å line (see Fig. 10). One of them included jet's footpoint, the other included the loop rope located above the central sunspots. After that, we calculated the average brightness for these areas at different times. The results of the last one are shown in Fig. 11. Thus, the jets and radio bursts associated with them preceded the CME and the X-ray flare, and they continued during and after it.

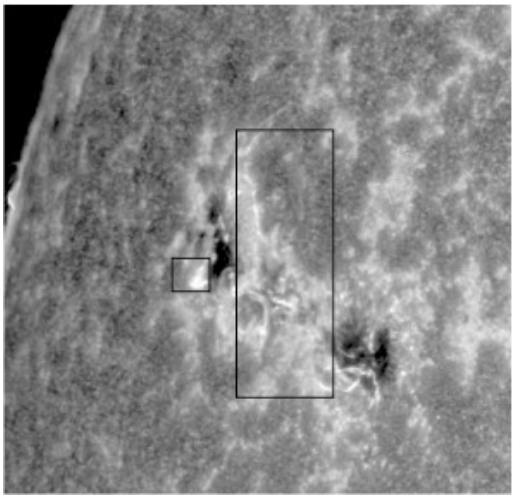


Figure 10 The AR 11302 image recorded in the 1600 Å line (SDO/AIA) on September 24, 2011 at 12:26 UT. The black frames indicate the areas in which the averages were taken.

4 Discussion and conclusions

Based on the results of this study, the following conclusions can be obtained:

1. In the AR 11302 on September 24, 2011 the complex magnetic configuration arose; in the tail sunspots the magnetic flux canceling was observed.
2. To the east and south-east of the tail sunspots there were high coronal loops, and above the central sunspots – the system of low loops.
3. Along the high loops, the EUV jets regularly erupted, both before the onset of the LDE-flare, and after it. The jets corresponded to type III radio bursts.
4. The high-energy mass CME, coinciding in the direction with jets, began earlier than the X-ray and chromospheric flares.
5. The CME consisted of two parts, one of which was observed earlier in time, and so it can be assumed that the so-called "cannibalism" of the CME took place.
6. The flare observed in Hα and 1600 Å lines spatially coincided with the rope of loops of different brightness located above the central sunspots.

Recurrent jets were the only eruptive phenomena in the chromosphere and the transition region before and during the LDE-flare being investigated. Since they started before the CME, it can be assumed that they were the cause or trigger of the CME (Liu et al. 2015). The fact that jets cause the disturbance in the upper corona is indicated by type III radio bursts, especially those recorded after 15:12 UT and 15:40 UT, when there were no other eruptive events.

As for the chromospheric one-band flares (Antalova, Jakimiec 1989), which usually occur with filament eruption, in our case, the appearance of this flare is most likely due to the interaction of the loop rope and the matter depositing after the CME. Note that on this day and the next few days after the LDE-flare, several more X-ray M

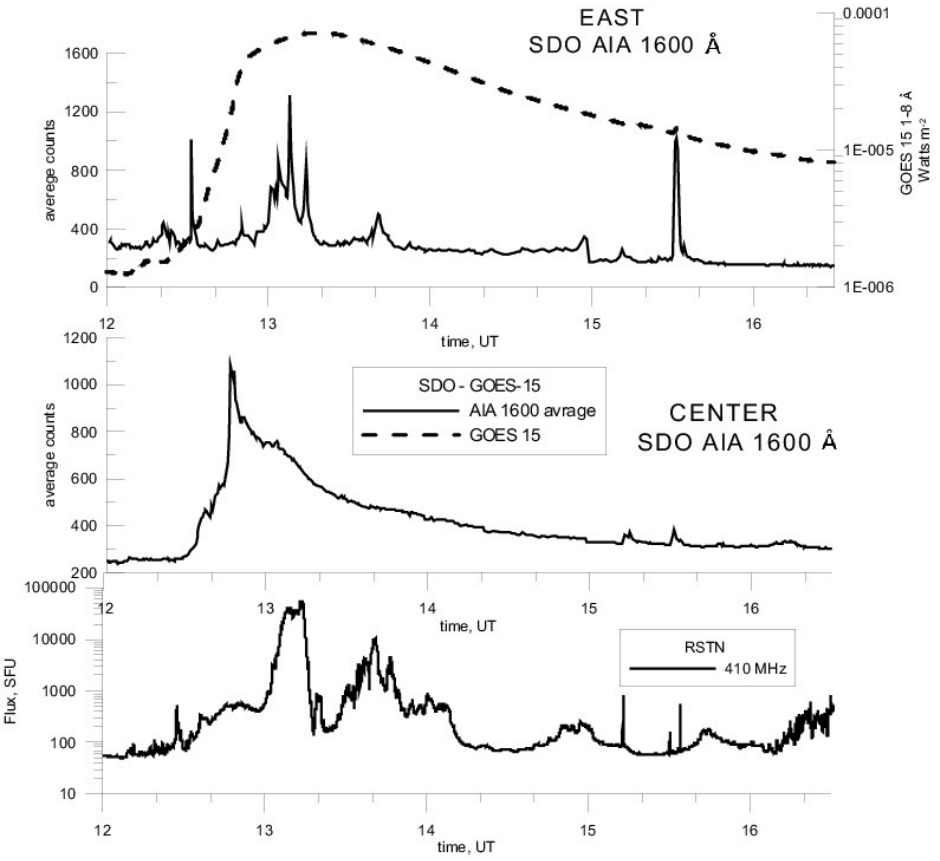


Figure 11 On the top panel the dashed line indicates the flux of soft X-ray (GOES-15 data). The solid line shows the data averaged over the eastern area in the Sun image in the 1600 Å line. The middle panel shows the data averaged over the central area, and on the bottom panel – the total flux in the radio range of 410 MHz (RSTN). Scales (left): average counts in top and middle panels, flux in the solar flux union (s.f.u.) in the bottom panel and the Universal Time (UT) in hours (below).

flares occurred in this AR, in the same rope, but they had a much shorter duration. This fact may indicate that magnetic reconnections can occur in the loop rope itself at low altitudes. A similar phenomenon is described in Cairns et al. (2018). And as the result, flares appear but the post-eruptive phase occurs in them only in the case of a large mass CME.

EUV jets are described in detail in Innes et al. (2016), Lim et al. (2016), Wyper, DeVore (2016), and Liu et al. (2015). Our study is in agreement with their models and observations, in particular, that jets occur at magnetic flux canceling sites, propagate along high coronal loops, are associated with type III radio bursts and can be CME triggers. The connection between chromospheric and coronal ejections with LDE-flares was discussed by the authors and their co-authors in Shakhovskaya, Livshits,

Chertok (2006), Shakhovskaya, Akhtemov (2013), Livshits et al. (2013), and also in Shibasaki (2002). They show that the subsequent fall of matter after the CME into the region of closed force lines, in particular, over the neutral magnetic field line, can support the post-eruptive system and its soft X-ray emission for a long time. In this case, reconnection of the magnetic force lines can play a large role in the places adjacent to the core of the flare (near the sunspots). While, at a considerable distance from the core of the flare, the effect of a fall in matter begins to predominate, this is especially pronounced in the case of the CME cannibalism. In this work, the example of specific events shows the connection of LDE-flares and EUV jets, where the CME acts as a connecting element.

Acknowledgements

The authors thank the SOHO/LASCO, SDO/AIA and HMI, GOES and the RSTN team the NASA/SDO, AIA, HMI science teams; the NASA STEREO/ SECCHI science and instrument teams; the USAF RSTN network, and LASCO on SOHO. SOHO is a project of international cooperation between ESA and NASA. We thank the team maintaining the CME Catalog at the CDAW Data Center by NASA and the Catholic University of America in cooperation with the Naval Research Laboratory for the open data used in the analysis. We are thankful to the referees for important remarks, which helped us to improve the paper.

References

Antalova, A., Ogir, M.B. (1988) Bull. Czechoslovakia Astron. Ins. 39, 97
Antalova, A., Jakimiec, M. (1989) Bull. Czechoslovakia Astron. Ins. 40, 311
Babin, A.N. (1974) Izv. Krym. Astrofiz. Obs. 52, 79
Babin, A.N., Koval', A.N. (1985) Izv. Krym. Astrofiz. Obs. 73, 3
Bein, B.M., Berkebile-Stoiser, S., Veronig, A.M., et al. (2012) ApJ 755, id. 44
Brueckner, G.E., Howard, R.A., Koomen, M.J., et al. (1995) Solar Phys. 162, 357
Cairns, I.H., Lobzin, V.V., Donea, A., et al. (2018) NatSR 8, id. 1676
Gopalswamy, N. (2003) Adv. Sp. Res. 314, 869
Grechnev, V., Uralov, A. M., Zandanov, V.G., et al. (2006) PASJ 58, 55
Guidice, D.A. (1979) Bull. Am. Astron. Soc. 11, 311
Guidice, D.A., Cliver, E.W., Barron, W.R., Kahler, S. (1981) Bull. Am. Astron. Soc. 13, 553
Howard, R.A., Moses, J.D., Vourlidas, A., et al. (2008) Sp. Sci. Rev. 136, 67
Innes, D.E., Buk, R., Guo, L.-J., Nitta, N. (2016) AN 337, 1024
Kaiser, M.L., Kucera, T.A., Davila, J.M., et al. (2008) Sp. Sci. Rev. 136, 5
Lemen, J.R., Title, A.M., Akin, D.J., et al. (2012) Solar Phys. 275, 17
Lim, E.-K., Yurchyshyn, V., Park, S.-H., et al. (2016) ApJ 817, id. 39
Liu, J. Wang, Y., Shen, C., et al. (2015) ApJ 813, id. 115
Livshits, M.A., Belov A.V., Eroshenko, E.A. et al. (2013) CosRe 51, 326 (Kosm. Is. 51, 326)

Scherrer, P.H., Schou, J., Bush, R.I., et al. (2012) Solar Phys. 275, 207.
Shakhovskaya, A.N., Livshits, M.A., Chertok, I.M. (2006) ARep 50, 1013 (AZh 83, 1128)
Shakhovskaya, A.N., Akhtemov, Z.S. (2013) Bull. Crimean Astrophys. Obs. 109, 86
Shibasaki, K. (2002) ApJ 567, L85
Wang, J., Shi, Z. (1993) Solar Phys. 143, 119
Wyper, P.F., DeVore, C.R. (2016) ApJ 820, id. 77